

We are IntechOpen, the world's leading publisher of Open Access books Built by scientists, for scientists

6,900

Open access books available

186,000

International authors and editors

200M

Downloads

Our authors are among the

154

Countries delivered to

TOP 1%

most cited scientists

12.2%

Contributors from top 500 universities



WEB OF SCIENCE™

Selection of our books indexed in the Book Citation Index
in Web of Science™ Core Collection (BKCI)

Interested in publishing with us?
Contact book.department@intechopen.com

Numbers displayed above are based on latest data collected.
For more information visit www.intechopen.com



Witnesses of Quantum Chaos and Nonlinear Kerr-Like Oscillator Model

Joanna K. Kalaga, Marcin W. Jarosik,
Wiesław Leoński and Radosław Szczęśniak

Additional information is available at the end of the chapter

<http://dx.doi.org/10.5772/intechopen.70747>

Abstract

Here, we present a brief insight into some current methods allowing for the detection of quantum chaos phenomena. In particular, we show examples of proposals of the parameters which could be applied as indicators of quantum-chaotic behavior and already were presented in the literature. We concentrate here on the quantum fidelity and the fidelity-like functions, defined for the wave functions describing system's evolution. The definition of the fidelity-like parameter also involves the operator of the mean number of photons/phonons. Discussing such parameter, we show here how it is possible to take into account in the discussion of quantum-chaotic systems simultaneously the behavior of the divergence of wave functions and the energy of the system represented by the mean number of photons/phonons. Next, we discuss entropy-type parameter which can also be a good candidate for the indicators of quantum chaos' phenomena. We show the ability of all considered here parameters to be witnesses of quantum-chaotic behavior for the systems of the quantum nonlinear Kerr-like oscillator—the classical counterpart of such system can exhibit chaotic evolution in its canonical form.

Keywords: quantum chaos, quantum nonlinear oscillator, Kerr-like oscillator, fidelity, entropy, photons, phonons

1. Introduction (some history)

The classical chaos phenomenon is related to the irregular and unpredictable evolution of nonlinear systems. What is important is that the behavior of such systems is determined, which means that time evolution of the system's state can be described by corresponding equations, usually in a form of nonlinear differential equations. The term “irregular evolution” is related to the nature of the dynamics of the system and is not related to the unpredictable

influence of the environment. The chaotic behavior exhibits itself in high sensitivity of system's evolution to the initial conditions. In fact, it refers to the situation when we are not able to determine the final state of a system when we have limited information concerning its initial state. On the other hand, when the initial state of the system is well defined, according to the principle of determinism, its final state should be well determined. However, for real systems, such ideal situation cannot be observed, as the initial conditions are always determined with some accuracy.

One of first papers describing the chaotic behavior of the studied systems was published at the end of the nineteenth century. In the years 1892–1899, Henri Poincaré published the work of *Les Méthodes Nouvelles de la Mécanique Céleste* [1], which attempts to answer the question: whether the solar system is stable? Poincaré studied the behavior of the reduced Hill model. This model consists of three bodies, which interact with gravity forces. Additionally, the mass of one of the bodies is so small that does not affect on the behavior of the other two. On the other hand, the other two bodies influence the behavior of the first one. Henri Poincaré, in his research, has obtained very complex trajectories of motion for small body, which we now call chaotic.

The great importance in chaos theory plays studies initiated by Kolmogorov [2] and continued by Arnold [3] and Moser [4]. Their studies concerned the integrable Hamiltonian systems and the influence of small perturbations on such systems. They have shown that when small perturbations are present in a dynamical system, some fraction of orbits in the phase space remains indefinite in some region of the space. That result is now known as KAM theorem.

In 1963, Lorenz [5] numerically studied a simple model of cellular convection (called Rayleigh-Bénard convection model) and discovered that all equations of motion are unstable and almost all are nonperiodic. He also paid attention to the phenomenon of the sensitivity of the system's evolution to the initial conditions. The system which models cellular convection consists of two horizontal plates and a liquid medium placed between them. The temperature of the top plate is lower than that measured at the surface of the bottom plate. For some values of the temperature difference ΔT , although we observe the convection rolls in the fluid, the state of the system remains stationary. By increasing ΔT , the fluid flow rate changes, and the behavior of the system becomes chaotic. In the following years, Rayleigh-Bénard convection was also studied by Ahlers and Behringer [6], Gollub and Benson [7], Libchaber and Maurer [8], and Bergé et al. [9]. The model analyzed by Lorenz can be applied to describe the behavior of various physical systems. For example, in 1975 Haken applied Lorenz model to explain the irregular spiking behavior of laser system [10].

The same time when Lorenz was studying the model of cellular convection, Ueda analyzed Duffing's model [11, 12] which describes a periodically excited damping system. Ueda observed that for some values of the amplitude of excitation force and the damping parameter system's oscillations become accidental. Further studies showed that damped oscillators, which are excited by a periodic force, for certain values of the parameters describing excitation, are sensitive to initial conditions.

In 1898, Hadamard studied the behavior of the geodesics on surfaces with constant negative curvature [13]. He proved that the motion along geodesic lines on negative curvature surfaces is unstable and this system exhibits sensitivity to initial conditions. That means that small change in initial direction of a geodesic entails large changes in predicted results after a long time. These studies were continued by Birkhoff [14]. In subsequent years successive systems were discussed in the context of chaotic behavior and their sensitivity to initial conditions. Nowadays, the chaos theory is applied to the discussions of a broad range, not necessarily physical problems, for instance, the motion of planets [15, 16], chemical reactions [17], medicine [18, 19], and others.

In the twentieth century, the new field of physics has been developed, including quantum mechanics. One of the main principles of quantum mechanics is proposed by Bohr, correspondence principle [20]. With accordance to it, when the value of the action associated with the energy of the system is much higher than the Planck constant, the quantum description of the system reduces to the classical one. In consequence, if for the classical counterpart of the quantum system we observe the transition to chaotic behavior, the similar effect should appear in the quantum system. However, such transitions appearing in quantum systems have the entirely different character from those originating in the classical ones. It can be explained as a result of the fact that the Schrödinger equation which describes the evolution of the quantum system is linear with respect to the wave function. In consequence, it gives periodic or quasi-periodic solutions which do not lead to the chaotic behavior in the classical sense. Additionally, as a result of the Heisenberg uncertainty principle, it is not possible to consider the trajectories in phase space, and the main feature of classical chaos cannot be observed. In quantum mechanics, all points in a $2n$ -dimensional space which are located in the volume smaller than \hbar^n are indistinguishable. Therefore, if the state of the system remains inside such region, when the system's dynamics is classically chaotic, in the quantum regime, such chaotic effects are not visible. Then, we cannot analyze the rate of separation of infinitesimally close trajectories known as the Lyapunov exponent. On the other hand, according to Bohr's correspondence principle when the Planck constant tends to zero, the results of quantum mechanics should correspond to the results of classical mechanics. According to that, the transition to the chaotic behavior of the classical system should lead to the appearance of the changes in dynamics of the quantum system. Therefore, when we study quantum chaos, we try to find some differences between the behavior of quantum systems for which classical counterpart exhibits regular evolution and quantum systems for which their classical counterparts are chaotic. Thus, one of the primary goals of the research in the field of quantum chaos is to find such parameters (witnesses) which allow for distinguishing between such two types of quantum behavior. For instance, the differences appearing in spectra of quantum-mechanical systems were predicted by Percival in 1973 [21] and then confirmed in 1979 by McDonald and Kaufman [22]. Those latter have studied the behavior of a particle which moves within the region confined inside rigid walls composed of two semicircles of radius r and two parallel segments of length d (see **Figure 1b**). Such system is called the *quantum billiard*, and its classical counterparts regularly behave when $d=0$ (**Figure 1a**). McDonald and Kaufman studied the distribution of distances $N(\Delta E)$ between two neighboring energy levels $\Delta E = E_{k+1} - E_k$. For a circular billiard ($d=0$), when $E=0$ the distribution $N(\Delta E)$ reaches its greatest value (**Figure 2**).

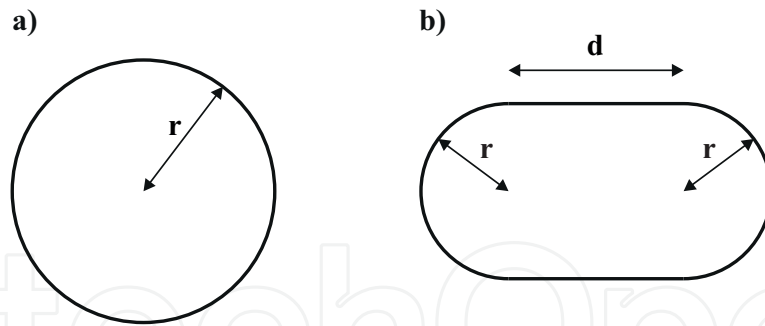


Figure 1. The billiard systems: (a) circular and (b) stadium.

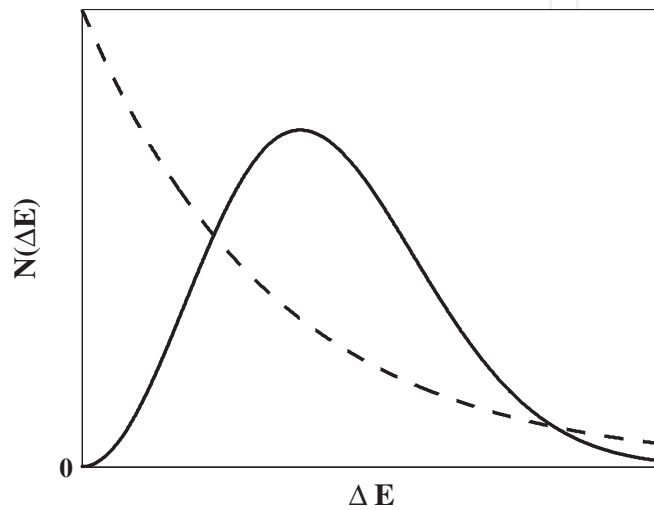


Figure 2. The distribution of distances between two neighboring energy levels $N(\Delta E)$ for circular billiard (dashed line) and stadium billiard (solid line).

When energy E increases, the value of $N(\Delta E)$ decreases. In consequence, we can observe the phenomenon called *attraction of energy levels* which can lead to their degeneracy. However, for stadium billiard ($d \neq 0$), the distribution $N(\Delta E)$ changes considerably. For $E=0$ it does not take its maximum value as we observed for the earlier case—it reaches its maximum for another value of the energy $E \neq 0$. That means that for the stadium billiard systems the phenomenon called *repulsion of energy levels* appears. At this point, we should also mention that similar result for the quantum Sinai's billiard was obtained by Bohigas et al. [23].

In 1984 Peres proposed a new way of studying the dynamics of quantum systems [24]. His method was based on the comparison of the evolution of the unperturbed system to that corresponding to the same system for which small perturbations Δ were applied into the Hamiltonian H . The state of the unperturbed system is described by the wave function Ψ_u , whereas Ψ_p represents the state corresponding to the perturbed Hamiltonian. To determine the distance between such two states, we need to calculate the scalar product of two corresponding to them wave functions and then define parameter

$$F = |\Psi_u(t)|\Psi_p(t)|, \quad (1)$$

which is called *fidelity*. At this point, one should mention that in the literature the fidelity is sometimes defined as squared modulus, not modulus itself. Moreover, especially in the papers dealing with condensed matter physics, the fidelity is called *Loschmidt echo* (for instance, see ([25] and the references quoted therein). Such quantity was applied for investigation of quantum-chaotic phenomena for the first times by Peres [24] and then by Weinstein et al. and Emerson et al. [26, 28]. The fidelity was also discussed in Ref. [27], where anharmonic oscillator models excited by ultrashort pulses were considered. For a quantum system whose classical counterpart shows regular behavior, we observe regular oscillations of the fidelity. However, when the classical counterpart of a quantum system exhibits a chaotic behavior, the evolution of the fidelity changes its character. It was shown in [26, 28] that in such a case the value of F decreases. The way in which such fidelity decays depends on the value of perturbation Δ . The methods of investigation of quantum-chaotic systems based on the fidelity were applied in studies of the dynamics of various quantum systems such as the quantum kicked top [26, 29], quantum nonlinear oscillator [27], particle kicked by a Gaussian beam [30], Josephson junction [31], etc.

2. The quantum nonlinear Kerr-like oscillator system: its quantum and classical evolution

To show the ability of discussed here parameters to describe quantum-chaotic phenomena, we need to choose a physical model which can exhibit quantum chaos' effects. The model should be a nonlinear type and allows to compare its quantum dynamics with its classical counterpart. We decided to discuss nonlinear Kerr-like oscillator systems. The models which we will apply are general enough to be applied in various fields. For instance, they can be applied to description nanomechanical resonators and various optomechanical systems [32–38], boson trapped in lattices [39–41], Bose-Hubbard chains [41, 42], circuit QED models [43, 44], etc.

The Hamiltonian for the anharmonic oscillator excited by a series of ultrashort pulses can be written as

$$\hat{H} = \hat{H}_{NL} + \hat{H}_K, \quad (2)$$

where the first part \hat{H}_{NL} describes “free” evolution of the oscillator during the time between two subsequent external pulses. \hat{H}_{NL} can be written with the use of boson creation and annihilation operators as

$$\hat{H}_{NL} = \frac{\chi}{2} (\hat{a}^\dagger)^2 \hat{a}^2. \quad (3)$$

The parameter χ appearing here describes nonlinearity of the oscillator. Here, we will assume for the convenience that $\chi=1$ and, then, other quantities will be expressed in units of χ . The second Hamiltonian \hat{H}_K is related to the interaction of the system with the external coherent pulses. It can be expressed in the following form:

$$\hat{H}_K = \varepsilon (\hat{a}^\dagger + \hat{a}) \sum_{k=1}^{\infty} \delta(t - kT), \quad (4)$$

where ε describes the strength of external excitation, whereas T denotes the duration of the time between two subsequent pulses (for the cases discussed here, we will assume that $T = \pi$). Appearing here Dirac-delta function models a single, infinitely short external pulse. In fact, every single pulse is much shorter than the time interval between two successive pulses but is sufficiently long to allow nonlinear system interact with the field.

As we neglect here all damping effects, the system's evolution can be described by unitary operators defined with the use of two Hamiltonians. We can notice that the whole evolution can be divided into two types of subsequent stages. Thus, for the moments of time, when $t = kT$ ($k = 1, 2, \dots$), the external pulses act on the oscillator. It is described by the Hamiltonian H_K . On the other hand, during the period between two subsequent pulses, the anharmonic oscillator evolves "freely," and such evolution is governed by H_{NL} . In consequence, we can define two unitary evolution operators \hat{U}_K and \hat{U}_{NL} , respectively. They are.

$$\hat{U}_K = e^{-i\varepsilon(\hat{a}^\dagger + \hat{a})} \quad (5)$$

and

$$\hat{U}_{NL} = e^{-i\chi T \hat{n}(\hat{n}-1)/2}, \quad (6)$$

where $\hat{n} = \hat{a}^\dagger \hat{a}$ is the photon number operator. Applying \hat{U}_{NL} and \hat{U}_K , we can define the operator \hat{U}_u transforming the wave function from that corresponding to the moment of time just after k th external pulses to that for the moment after $(k + 1)$ th one. Such defined time evolution operator allows for a so-called quantum mapping of the system. For unperturbed system \hat{U}_u has the following form:

$$\hat{U}_u = e^{-i\varepsilon(\hat{a}^\dagger + \hat{a})} e^{-i\chi T \hat{n}(\hat{n}-1)/2}. \quad (7)$$

When we apply the perturbation Δ , corresponding to it evolution operator \hat{U}_p is defined as

$$\hat{U}_p = e^{-i(\varepsilon + \Delta)(\hat{a}^\dagger + \hat{a})} e^{-i\chi T \hat{n}(\hat{n}-1)/2}. \quad (8)$$

Next, to find solutions we need to choose initial state of the system. Here, we will assume that the system's evolution starts from the vacuum state $|\Psi(0)\rangle$. Thus, we are in the position to find two wave functions appearing in the definition of fidelity. After the k -fold operation of the evolution operators onto the initial state, we obtain the wave functions (perturbed and unperturbed ones) corresponding to the moments of time just after the k th pulse. They are

$$|\Psi_u(k)\rangle = \left(\hat{U}_u \right)^k |\Psi(0)\rangle \quad (9)$$

and

$$|\Psi_p(k)\rangle = (\hat{U}_p)^k |\Psi(0)\rangle, \quad (10)$$

respectively. Finally, the modulus of the scalar product of such calculated wave functions gives the fidelity defined in Eq. (1).

As we have mentioned earlier, it is necessary to determine the regions for which the classical counterpart of our model exhibits regular or chaotic dynamics. Therefore, we will follow the path shown in [45]. First, we will find the solution for the annihilation operator and, then, replace the operators appearing there by appropriate complex numbers. Such solution will allow drawing a bifurcation diagram for the classical system.

We remember that during the time between two subsequent pulses the energy is conserved and the total number of photons is constant. Therefore, we can write the equation describing the time evolution of \hat{a} for such period of time:

$$\frac{d\hat{a}}{dt} = \frac{1}{i\hbar} [\hat{a}, \hat{H}_{NL}], \quad (11)$$

and it has the solution of the form

$$\hat{a}(\tau) = e^{-i\chi\hat{a}^\dagger\hat{a}\tau}\hat{a}. \quad (12)$$

To transform such determined annihilation operator from that corresponding to the moment of time just before a single pulse to that just after it, we can use \hat{U}_K defined in Eq. (8). Due to the fact that \hat{U}_K is the displacement operator, the recurrence formula transforming \hat{a} from the moment of time just after k th pulse to that after $(k+1)$ th one can be written as

$$\hat{a}_{k+1} = e^{-i\chi(\hat{a}_k^\dagger + i\varepsilon)(\hat{a}_k - i\varepsilon)T}(\hat{a}_k - i\varepsilon). \quad (13)$$

We can replace \hat{a} (\hat{a}^\dagger) by complex numbers α (α^*), now. In consequence, we get the following equation allowing for finding classical maps:

$$\alpha_{k+1} = (\alpha_k - i\varepsilon)e^{-i(\chi|\alpha_k - i\varepsilon|^2)T}. \quad (14)$$

The classical energy of the system is determined by $|\alpha|^2$, and, now, we can draw a bifurcation diagram for the classical nonlinear system. Thus, **Figure 3** shows such diagram plot for various values of the strength of external pulses ε . We see that the character of our system's dynamic depends on the value of this parameter—the evolution of the classical system is regular for $\varepsilon < 0.344$ and $0.362 < \varepsilon < 0.47$ and when $0.344 < \varepsilon < 0.362$ and $0.47 < \varepsilon$, the classical system exhibits chaotic evolution.

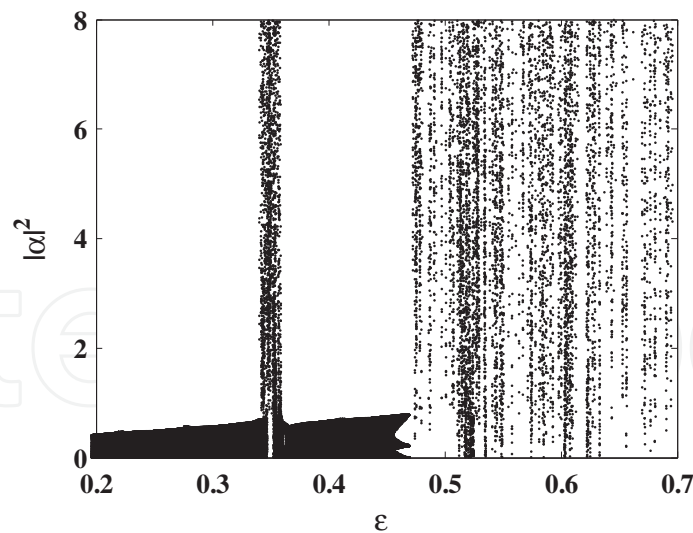


Figure 3. The bifurcation diagram showing the dependence of the average energy $|\alpha|^2$ on the excitation strength ε . The system is not damped, and the time between two subsequent pulses is assumed to be $T=\pi$.

3. Witnesses of quantum chaos

3.1. The fidelity

From the bifurcation diagram, we know for which values of external excitations ε the evolution of the classical counterpart of the quantum system is regular and for which it is chaotic. Choosing the appropriate values of ε , we can examine the time evolution of the fidelity:

$$F(k) = |\langle \Psi(0) | \hat{U}_u^k \hat{U}_p^k | \Psi(0) \rangle|, \quad (15)$$

where \hat{U}_u and \hat{U}_p are already defined in Eqs. (7) and (8). We concentrate here on the behavior of $F(k)$ in a long-time limit.

In **Figure 3** one can see that four regions of different characters of the system's dynamics appear there. There are regular area for $\varepsilon < 0.344$, narrow chaotic band for $0.344 < \varepsilon < 0.362$, second regular area for $0.362 < \varepsilon < 0.47$, and area of deep chaos for $\varepsilon > 0.47$. Therefore, we choose four values of ε to examine the behavior of $F(k)$ in all four areas. They are $\varepsilon = \{0.2; 0.35; 0.45; 0.65\}$, and for such values of ε , the time evolution of the fidelity is presented in **Figure 4**. In addition, we assumed here that the perturbation parameter $\Delta = 0.001$.

Figure 4a shows the time evolution of fidelity for $\varepsilon = 0.2$. For this value of ε , the dynamics of the classical counterpart of the quantum system is regular. We can observe here that the value of $F(k)$ changes in time periodically from zero to unity. We see that the both amplitude and period of oscillations remain constant even for the long-time limit. Here, the value of the period of oscillations is equal to 3178 pulses (after such number of pulses $F(k)$ reaches its initial value $F(0) = 1$). The similar situation we observe for $\varepsilon = 0.45$ (see **Figure 4c**). In bifurcation diagram, this value of the external excitation corresponds to the second regular region

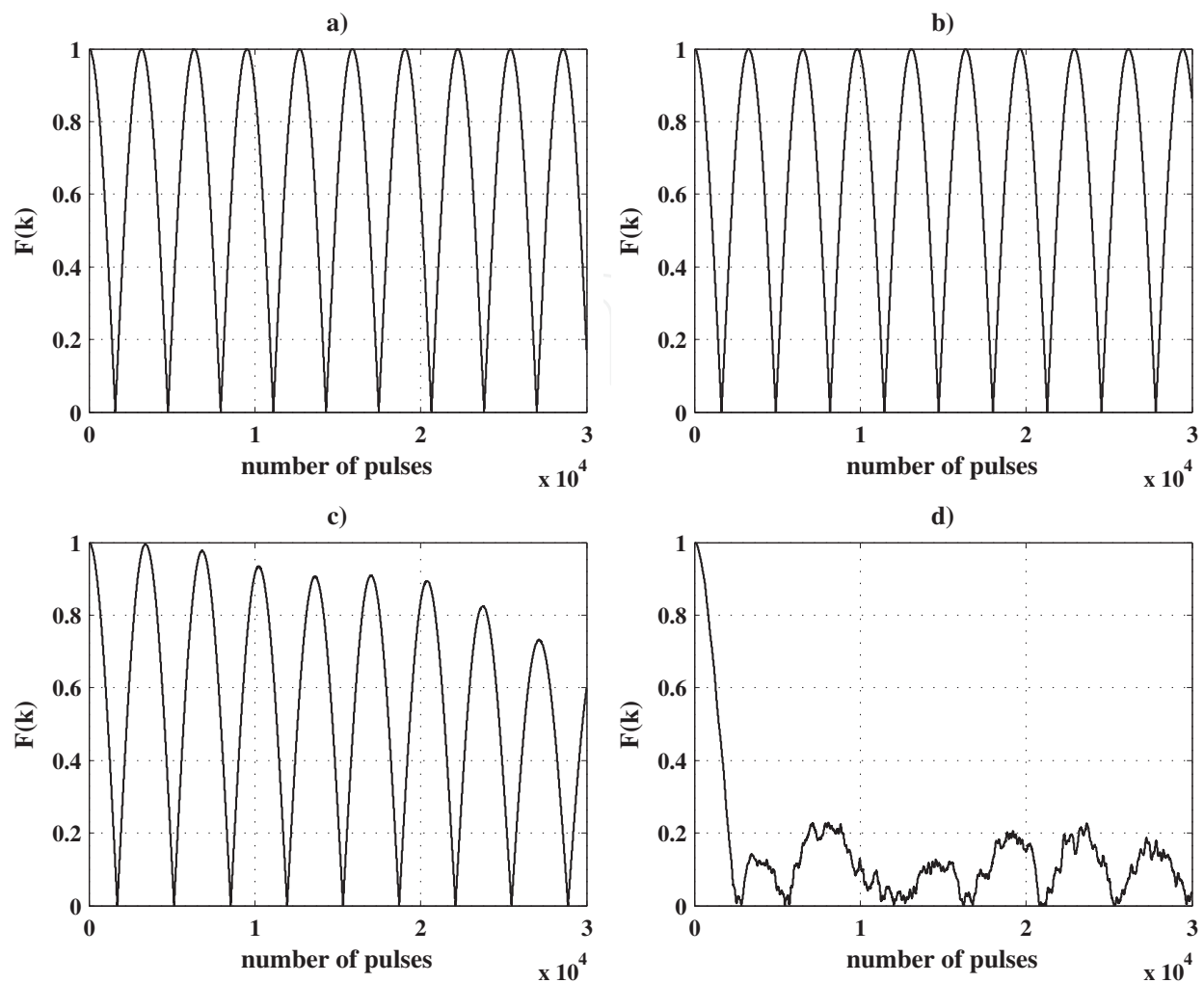


Figure 4. The fidelity versus the number of pulses for (a) $\varepsilon=0.2$, (b) $\varepsilon=0.35$, (c) $\varepsilon=0.45$, and (d) $\varepsilon=0.65$. The perturbation parameter $\Delta=0.001$.

(band). The amplitude of oscillations is slowly modulated, so we observe beating effect. This effect appears as a result of the proximity of chaotic region which affects oscillations of F , and additional frequency appears in the evolution. Analogously to the case (a), the fundamental oscillations of the fidelity are regular, and its period is constant and equal to 3414 pulses (the period differs slightly from that of case (a)). Appearing of additional frequencies is related to the bifurcations which appear for the values of ε slightly smaller than that for that corresponding to the deep chaos border.

The case when $\varepsilon=0.35$ seems to be more attractive. Such value of the external excitation corresponds to the chaotic band which is located between two regular areas. The same as for the case when $\varepsilon=0.2$; the fidelity changes periodically from zero to unity. Thus, we could conclude that we are in the regular area, and the question arises: why the evolution of the fidelity for $\varepsilon=0.35$ is practically the same, as that for $\varepsilon=0.2$? Probably, such evolution is strongly influenced by the neighborhood of the two regular areas which we see in the bifurcation diagram. Moreover, such behavior of the system becomes more clear when we plot the map defined in a two-dimensional phase space for the classical case and, then, overlap it with

Husimi Q-function. Q-Function is one of the quasi-probabilities which gives the information concerning system's quantum state presented in a phase space (for the discussion of various quasi-probabilities usually applied in quantum optics, see, for instance, [46] *and the references quoted therein*). We should note at this point that the parameter of mutual information which was also proposed as a tool which can be applied in a finding of the quantum-chaotic behavior [47] is derived with the use of Husimi Q-function. Moreover, Q-function is not the only one quasi-probability function which can be applied in an investigation in that field. For instance, in [48] the parameter derived on the basis of the Wigner quasi-probability function was also considered in a context of finding quantum chaos witnesses.

Figure 5 shows the classical map (represented by dots) and contour plot of Q-function (dashed lines). We see that the main peak of Q-function (and the greatest probability) is placed in the region corresponding to the regular trajectories in the phase plane. This fact explains why the time evolution of F exhibits regular character.

For $\varepsilon = 0.65$ (this situation corresponds to the area of deep chaos in the bifurcation diagram) the behavior of F completely differs from the previous cases (a)–(c) in **Figure 4**. When the system starts its evolution, we observe decay of the fidelity. The character of such initial vanishing of F was discussed in [26], where it was shown that it changes at the border of chaotic region and, thus, it can be applied as the witness of quantum chaos. Let us concentrate on the time evolution of F for the longer times. So, apart from the initial decay, we can see that the fidelity evolves in an irregular way in the long-time regime. Such irregularity appears when the values of excitations correspond to the area of deep chaos in the bifurcation diagram.

For each case discussed here, the perturbation parameter Δ is small, according to the perturbation theory. Therefore, the initial decay of the fidelity is described by the Gaussian functions [26]. This means that the decay of F can be characterized by the function $\exp(-const \cdot t^2)$. The rate of decay changes with the value of the external excitations. **Figure 6** shows how many

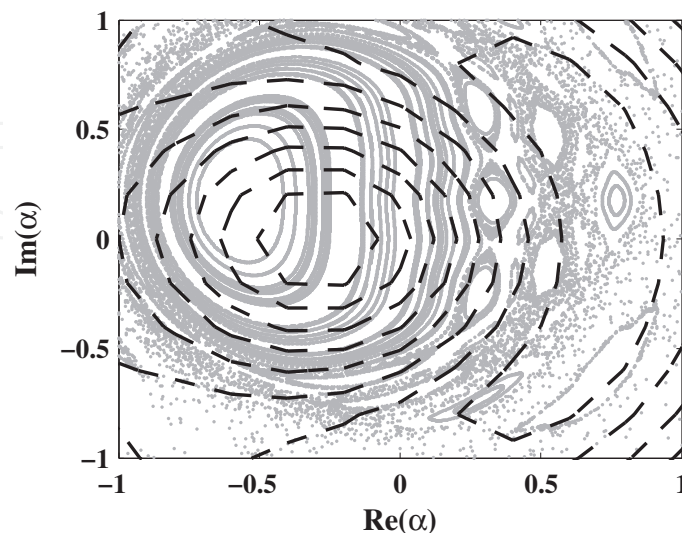


Figure 5. Classical map (dots) overlapping the contour plot of Q-function (dashed lines). We assume here that $\varepsilon = 0.35$. The remaining parameters are the same as those for **Figure 4**.

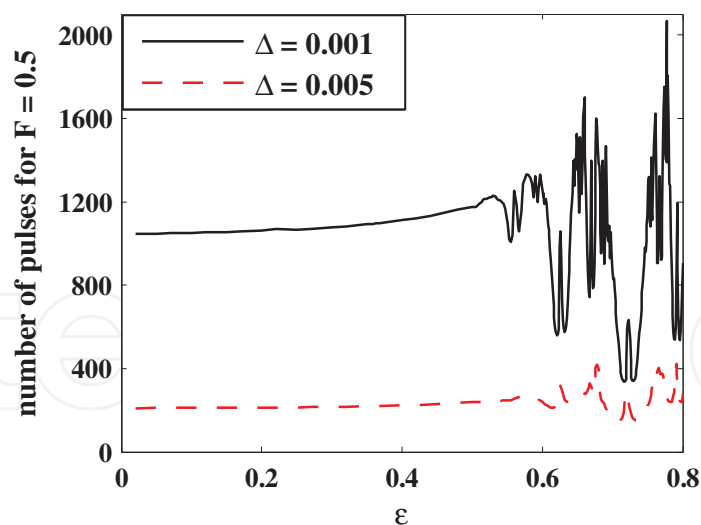


Figure 6. The number of pulses for which the fidelity reaches 0.5 for the first time, as a function of the strength of excitation for two values of the perturbation parameter Δ .

pulses are necessary for the fidelity to get the value 0.5 for the first time, for various values of the strength of the external excitation ε . We see that when ε increase, the time (in fact, the number of the pulses) for which F reaches 0.5 also increases, and, hence, the rate of initial decay of the fidelity decreases. We observe such relation between the decay rate and the strength of the external pulse for $\varepsilon < 0.47$ (it corresponds to both areas of regular motion and the narrow chaotic band in the bifurcation diagram). On the other hand, for the excitations corresponding to the region of deep chaos, the rate of fidelity decay changes irregularly. We observe similar behavior for various values of perturbation parameter Δ . However, when Δ increases, the time of decay becomes shorter, and the rate of fidelity decay is greater (see **Figure 6**). What is important is that when the values of the perturbation parameter become greater and greater, the transition to the phase of its irregular changes with ε is less pronounced, so it is harder to detect the edge of chaotic behavior from discussed dependence.

3.2. Entropic parameter ε

Entropic measures, especially the Kolmogorov entropy, are the most relevant parameters of characterizing chaotic dynamics [49]. Therefore, we will define here the entropy-like quantity ε to show how it could be applied in quantum chaos detection. What is important is that ε will be defined for the quantum, not a classical model.

Thus, first, we calculate the Fourier transform $F(k)$:

$$F(\omega) = \sum_k F(t) e^{-i\omega t} dt. \quad (16)$$

We applied here discrete transform due to the discrete character of the system's evolution which is influenced by the train of ultrashort external pulses. Then, we calculate the power spectrum $P(\omega) = |F(\omega)|^2$, and after its proper normalization, we define the entropy-like parameter ε in the form

$$E = - \sum_{\omega} P_N(\omega) \log (P_N(\omega)). \quad (17)$$

Thus, **Figure 7** shows how the value of ε depends on the strength of external excitation ε . We see that when the dynamics of the classical counterpart of our system is regular, the value of the parameter ε changes slightly with increasing ε . For strengths of the external excitation corresponding to the border of deep chaos, the value of ε increases rapidly. For even higher values of ε , when the classical system exhibits purely chaotic behavior, the value of the parameter ε increases, and, additionally, irregular oscillations appear with increasing ε . This result seems to be very promising. As for classical systems, the bifurcation diagram allows us to determine when it exhibits regular, or chaotic, evolution; the character of quantum system's dynamics could be confirmed by the application of the parameter defined in Eq. (17). The procedure discussed here to other parameters, for instance, Kullback–Leibler quantum divergence [50], is also a worth considering application.

3.3. The fidelity-like parameter

In the bifurcation diagram, we showed the values of $|\alpha|^2$ calculated for the long-time limit and corresponding to various values of ε . The classical value of $|\alpha|^2$ corresponds to the mean number of photons in the quantum picture. From another side, the fidelity $F(k)$ does not contain any information concerning the energy or, equivalently, numbers of photons for considered system. Thus, there is a need to define such parameter that would contain the information concerning both divergence of wave function and energy of the system. Therefore, we will discuss here the fidelity-like parameter $F_n(k)$ which could be not only a good witness of the divergence of two wave functions in Hilbert space but also contain the information concerning the mean number of photons. The definition of $F_n(k)$ should involve the operator $\hat{n} = \hat{a}^\dagger \hat{a}$ and two wave functions (one corresponding to the perturbed system and second for the unperturbed

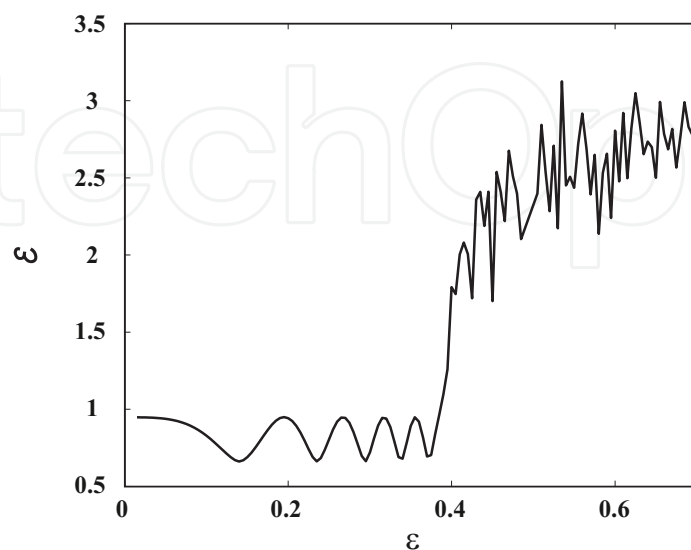


Figure 7. The entropic-like quantity ε versus the strength of external excitation ε .

one). Here, we discuss one of the parameters which its definition fulfills such requirements. Its definition can be written as [51]

$$F_n(k) = |\langle \Psi(0) | \hat{U}_u^k (\hat{a}^\dagger \hat{a}) \hat{U}_p^k | \Psi(0) \rangle|. \quad (18)$$

The parameter F_n gives us the possibility to directly compare the behavior of F_n with the information obtained from the bifurcation diagram. Analogously to the cases discussed earlier (see the discussion concerning the fidelity $F(k)$), we will analyze here four cases for which the external force takes the values $\varepsilon = \{0.2; 0.35; 0.45; 0.65\}$. They correspond to the four different areas in the bifurcation diagram shown in **Figure 3**. And thus, **Figure 8** depicts the time evolution of $F_n(k)$ (solid lines) and, additionally, for subfigures (a) and (b), previously defined fidelity $F(k)$ (dashed line).

When $\varepsilon = 0.2$, which corresponds to the regular evolution of the classical system, the value of F_n oscillates regularly (**Figure 8a**). Those oscillations are modulated, and we observe a beating

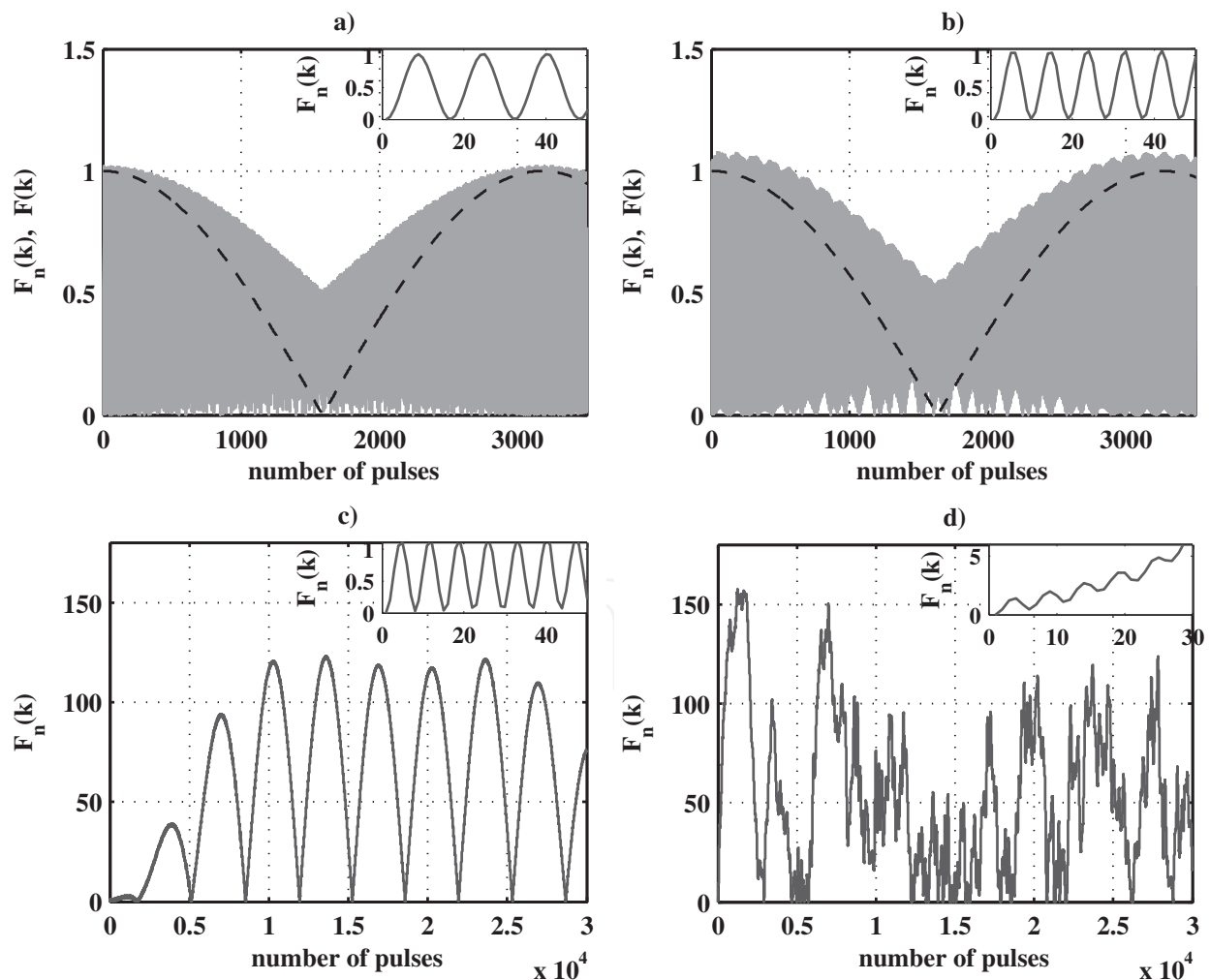


Figure 8. The fidelity-like parameter $F_n(k)$ (solid line) and fidelity $F(k)$ (dashed line) versus the number of pulses for (a) $\varepsilon = 0.2$, (b) $\varepsilon = 0.35$, (c) $\varepsilon = 0.45$, and (d) $\varepsilon = 0.65$. In the inset we have shown F_n in an extended timescale.

effect in the longer timescale. Such beating effect is related to the presence of two frequencies. The first of them corresponds to the low-frequency changes which we already observed for the fidelity (dashed line). The second frequency corresponds to the oscillations of the mean number of photons. As we see, the parameter $F_n(k)$ combines the features of the fidelity and the average number of photons.

For the case when $\varepsilon = 0.35$, the fidelity-like parameter $F_n(k)$ changes regularly (see **Figure 8b**). The same as for $\varepsilon = 0.2$, the time evolution of $F_n(k)$ is determined by two frequencies. The first frequency has the same value as the frequency of oscillation of fidelity. The second is related to oscillation of the mean number of photons. The same as for the case discussed previously and depicted in **Figure 4**, despite the presence of the chaotic band in the bifurcation diagram, all oscillations appearing in **Figure 8b** are of the regular character. Obviously, the regular changes in the time evolution of F_n are observed when $\varepsilon = 0.45$, as well (**Figure 8c**). However, for $\varepsilon = 0.45$ the time dependence of $F_n(k)$ is not clear like that discussed in the previous two cases. It is a result of the appearance of additional frequencies because, here, when $\varepsilon = 0.45$, we are in the vicinity of the chaotic region.

In contrast, when $\varepsilon = 0.65$ (chaotic area in the bifurcation diagram), the behavior of the $F_n(k)$ differs from all previous cases. In the beginning, we observe a characteristic increase of the value of F_n . Moreover, apart from the initial rise in the value of the fidelity-like parameter, we see its irregular variations. Contrary to the characteristic initial decay of the fidelity $F(k)$, which rate depends on the value of perturbation Δ , the fidelity-like parameter $F_n(k)$ exhibits initial rise. In **Figure 9** we present the first stages of time evolution of $F_n(k)$ for various values of Δ . For very early stages of the evolution, the growth of F_n is almost identical for all values of Δ . However, for the next moments of time, the rate of increase becomes damped for the cases of weak perturbation.

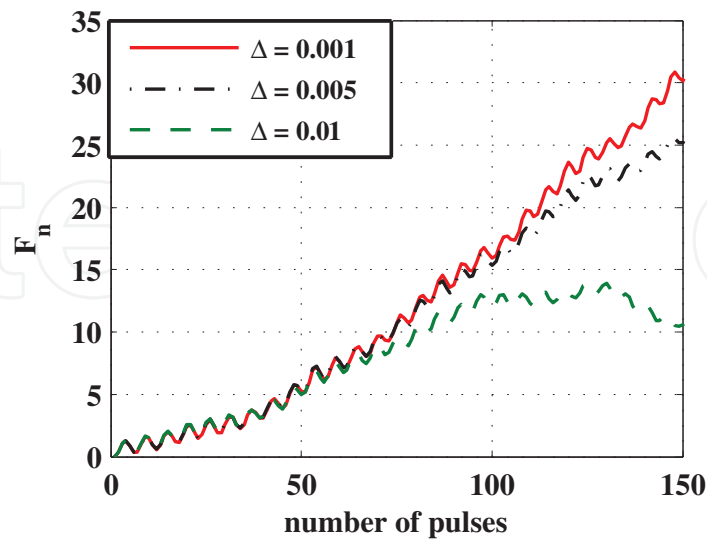


Figure 9. The initial rise of the fidelity-like parameter $F_n(k)$ for various values of the perturbation parameter Δ .

4. Conclusion

We have discussed here some proposals for the witnesses of quantum-chaotic behavior. In particular, we considered such parameters as the quantum fidelity and the fidelity-like parameter which characterizes not only the divergence of the wave functions but also the energy of the system. Moreover, the entropic witness describing the chaotic evolution of the fidelity (in a classical sense) was presented here. We discussed all those parameters in a context of their ability of detection of quantum-chaotic behavior. Using the exemplary system of quantum Kerr-type oscillators excited by a train of ultrashort pulses, we have shown how all presented here witnesses could be applied in detection of quantum chaos phenomena. We have shown how they are sensitive to the chaotic behavior when we are dealing with narrow chaotic bands and regions of deep chaos. We believe that we succeed here to show that considered here parameters are not only good witnesses of quantum chaos but also seem to be (with applied here methods) a good starting point in defining other quantities allowing for investigation of quantum chaos.

Author details

Joanna K. Kalaga¹, Marcin W. Jarosik², Wiesław Leoński^{1*} and Radosław Szczęśniak²

*Address all correspondence to: w.leonski@if.uz.zgora.pl

1 Quantum Optics and Engineering Division, Faculty of Physics and Astronomy, University of Zielona Góra, Zielona Góra, Poland

2 Institute of Physics, Częstochowa University of Technology, Częstochowa, Poland

References

- [1] Poincaré H. *Les Méthodes Nouvelles de la Mécanique Celeste*. Paris: Gauthier-Villars; 1892-1899
- [2] Kolmogorov AN. On conservation of conditionally periodic motions for a small change in Hamilton's function. *Doklady Akademii Nauk SSSR*. 1954;**98**:527-530
- [3] Arnold VI. Proof of a theorem by A. N. Kolmogorov on the invariance of quasi-periodic motions under small perturbations of the Hamiltonian. *Russian Mathematical Surveys*. 1963;**18**(5):13-40
- [4] Moser JK. Convergent series expansions for quasi-periodic motions. *Mathematische Annalen*. 1967;**169**:136-176

- [5] Lorenz EN. Deterministic nonperiodic flow. *Journal of the Atmospheric Sciences*. 1963;**20**(2):130-141. DOI: 10.1175/1520-0469(1963)020<0130:DNF>2.0.CO;2
- [6] Ahlers G, Behringer RP. Evolution of turbulence from the Rayleigh-Bénard instability. *Physical Review Letters*. 1978;**40**:712-716. DOI: 10.1103/PhysRevLett.40.712
- [7] Gollub JP, Benson SV. Many routes to turbulent convection. *Journal of Fluid Mechanics*. 1980;**100**(3):449-470. DOI: 10.1017/S0022112080001243
- [8] Libchaber A, Maurer J. Une Expérience de Rayleigh-Bénard en géométrie réduite: multiplication, accrochage et démultiplication de fréquences. *Le Journal de Physique Colloques*. 1980;**41**(C3):51-56. DOI: 10.1051/jphyscol:1980309
- [9] Bergé P, Dubois M, Manneville P, Pomeau Y. Intermittency in Rayleigh-Bénard convection. *Journal de Physique Lettres*. 1980;**41**:341-345. DOI: 10.1051/jphyslet:019800041015034100
- [10] Haken H. Analogy between higher instabilities in fluids and lasers. *Physics Letters A*. 1975;**53**(1):77-78. DOI: 10.1016/0375-9601(75)90353-9
- [11] Ueda Y. Randomly transitional phenomena in the system governed by Duffing's equation. *Journal of Statistical Physics*. 1979;**20**(2):181-196. DOI: 10.1007/BF01011512
- [12] Ueda Y. *Steady Motions Exhibited by Duffing's Equation: A Picture Book of Regular and Chaotic Motions, New Approaches to Nonlinear Problems in Dynamics*. Philadelphia: SIAM; 1980
- [13] Hadamard J. Les surfaces à courbures opposées et leurs lignes géodésiques. *Journal de Mathématiques Pures et Appliquées*. 1898;**4**:27-74
- [14] Birkhoff GD. On the periodic motions of dynamical systems. *Acta Math*. 1927;**50**:359-379. DOI: 10.1007/BF02421325
- [15] Hartley K. Solar system chaos. *Astronomy*. 1990;**18**:34-39
- [16] Thuan TX. *Chaos in the Cosmic Machinery, and Uncertainty in Determinism, in Chaos and Harmony: Perspectives on Scientific Revolution of Twentieth Century*. Oxford: Oxford University Press; 2001
- [17] Field RJ, Györgyi L. *Chaos in Chemistry and Biochemistry*. Singapore: World Scientific Publishing Co. Pte. Ltd.; 1993
- [18] Żebrowski JJ, Popławska W, Baranowski R. Entropy, pattern entropy, and related methods for the analysis of data on the time intervals between heartbeats from 24-h electrocardiograms. *Physical Review E*. 1994;**50**:4187-4205. DOI: 10.1103/PhysRevE.50.4187
- [19] Amaral LAN, Goldberger AL, Ivanov PC, Stanley HE. Scale-independent measures and pathologic cardiac dynamics. *Physical Review Letters*. 1998;**81**:2388-2391. DOI: 10.1103/PhysRevLett.81.2388
- [20] Bohr N. Niels Bohr—Collected Works, the Correspondence Principle (1918–1923). Vol. 3. In: Rosenfeld L, Rud Nielsen J, editors. North Holland; 1976. DOI: 10.1016/S1876-0503(08)70081-1

- [21] Percival IC. Regular and irregular spectra. *Journal of Physics B*. 1973;**6**(9):L229
- [22] McDonald SW, Kaufman AN. Spectrum and eigenfunctions for a hamiltonian with stochastic trajectories. *Physical Review Letters*. 1979;**42**:1189-1191. DOI: 10.1103/PhysRevLett.42.1189
- [23] Bohigas O, Giannoni MJ, Schmit C. Characterization of chaotic quantum spectra and universality of level fluctuation laws. *Physical Review Letters*. 1984;**52**:1-4. DOI: 10.1103/PhysRevLett.52.1
- [24] Peres A. Stability of quantum motion in chaotic and regular systems. *Physical Review A*. 1984 Oct;**30**:1610-1615. DOI: 10.1103/PhysRevA.30.1610
- [25] Woźniak D, Drzewiński A, Kamieniarz G. Quantum chaos systems and fidelity. *Acta Physica Polonica A*. 2016;**130**(6):1395-1400. DOI: 10.12693/APhysPolA.130.1395
- [26] Weinstein YS, Lloyd S, Tsallis C. Border between regular and chaotic quantum dynamics. *Physical Review Letters*. 2002;**89**:214101. DOI: 10.1103/PhysRevLett.89.214101
- [27] Kowalewska-Kudłaszyk A, Kalaga JK, Leoński W. Long-time fidelity and chaos for a kicked nonlinear oscillator system. *Physics Letters A*. 2009;**373**(15):1334-1340. DOI: 10.1016/j.physleta.2009.02.022
- [28] Weinstein YS, Emerson J, Lloyd S, Cory D. Fidelity decay saturation level for initial eigenstates. *Quantum Information Processing*. 2002;**1**(6):439-448. DOI: 10.1023/A:1024018431394
- [29] Prosen T, Znidaric M. Stability of quantum motion and correlation decay. *Journal of Physics A: Mathematical and General*. 2002;**35**(6):1455
- [30] Krivolapov Y, Fishman S, Ott E, Antonsen TM. Quantum chaos of a mixed open system of kicked cold atoms. *Physical Review E*. 2011;**83**:016204. DOI: 10.1103/PhysRevE.83.016204
- [31] Pozzo EN, Domínguez D. Fidelity and quantum chaos in the mesoscopic device for the josephson flux qubit. *Physical Review Letters*. 2007;**98**:057006. DOI: 10.1103/PhysRevLett.98.057006
- [32] Bose S, Jacobs K, Knight PL. Preparation of nonclassical states in cavities with a moving mirror. *Physical Review A*. 1997;**56**:4175-4186. DOI: 10.1103/PhysRevA.56.4175
- [33] Jacobs K. Engineering quantum states of a Nanoresonator via a simple auxiliary system. *Physical Review Letters*. 2007;**99**:117203. DOI: 10.1103/PhysRevLett.99.117203
- [34] Stobińska M, Milburn GJ, Wódkiewicz K. Wigner function evolution of quantum states in the presence of self-Kerr interaction. *Physical Review A*. 2008;**78**:013810. DOI: 10.1103/PhysRevA.78.013810
- [35] Liu YX, Miranowicz A, Gao YB, Bajer J, Sun CP, Nori F. Qubit-induced phonon blockade as a signature of quantum behavior in nanomechanical resonators. *Physical Review A*. 2010;**82**:032101. DOI: 10.1103/PhysRevA.82.032101

- [36] Rabl P. Photon blockade effect in optomechanical systems. *Physical Review Letters*. 2011;**107**:063601. DOI: 10.1103/PhysRevLett.107.063601
- [37] Wang H, Gu X, Liu YX, Miranowicz A, Nori F. Tunable photon blockade in a hybrid system consisting of an optomechanical device coupled to a two-level system. *Physical Review A*. 2015;**92**:033806. DOI: 10.1103/PhysRevA.92.033806
- [38] Kalaga JK, Kowalewska-Kudłaszyk A, Leoński W, Barasiński A. Quantum correlations and entanglement in a model comprised of a short chain of nonlinear oscillators. *Physical Review A*. 2016;**94**:032304. DOI: 10.1103/PhysRevA.94.032304
- [39] Wu L, Miranowicz A, Wang X, Liu Y, Nori F. Perfect function transfer and interference effects in interacting boson lattices. *Physical Review A*. 2009;**80**:012332. DOI: 10.1103/PhysRevA.80.012332
- [40] Barasiński A, Leoński W, Sowiński T. Ground-state entanglement of spin-1 bosons undergoing superexchange interactions in optical superlattices. *Journal of the Optical Society of America B: Optical Physics*. 2014;**31**(8):1845-1852. DOI: 10.1364/JOSAB.31.001845
- [41] Islam R, Ma R, Preiss PM, Tai ME, Lukin A, Rispoli M, et al. Measuring entanglement entropy in a quantum many-body system. *Nature*. 2015;**528**:77. DOI: 10.1038/nature15750
- [42] Preiss P, Ma R, Tai M, Lukin A, Rispoli M, Zupancic P, et al. Strongly correlated quantum walks in optical lattices. *Science*. 2015;**347**:1229-1233. DOI: 10.1126/science.1260364
- [43] Boissonneault M, Gambetta JM, Blais A. Dispersive regime of circuit QED: Photon-dependent qubit dephasing and relaxation rates. *Physical Review A*. 2009;**79**:013819. DOI: 10.1103/PhysRevA.79.013819
- [44] Rebić S, Twamley J, Milburn GJ. Giant kerr nonlinearities in circuit quantum electrodynamics. *Physical Review Letters*. 2009;**103**:150503. DOI: 10.1103/PhysRevLett.103.150503
- [45] Leoński W. Quantum and classical dynamics for a pulsed nonlinear oscillator. *Physica A: Statistical Mechanics and its Applications*. 1996;**233**:365-378. DOI: 10.1016/S0378-4371(96)00250-6
- [46] Gerry CC, Knight PL. *Introductory Quantum Optics*. Cambridge: Cambridge University Press; 2005
- [47] Kalaga JK, Leoński W, Kowalewska-Kudłaszyk A. System of nonlinear quantum oscillator and quantum correlations—Proposal for quantum chaos indicator. *Proceedings of SPIE*. 2014;**9441**:94410W
- [48] Kowalewska-Kudłaszyk A, Kalaga JK, Leoński W. Wigner-function nonclassicality as indicator of quantum chaos. *Physical Review E*. 2008;**78**:066219-066211
- [49] Schuster HG, Just W. *Deterministic Chaos—An Introduction*. Weinheim: Wiley-VCH Verlag; 2005

- [50] Kowalewska-Kudłaszyk A, Kalaga JK, Leoński W, Cao LV. Kullback-Leibler quantum divergence as an indicator of quantum chaos. *Physics Letters A*. 2012;**376**:128012-128086
- [51] Kalaga JK, Leoński W. Two proposals of quantum chaos indicators related to the mean number of photons: Pulsed Kerr-like oscillator case. *Proceedings of SPIE*. 2016;**10142**: 101421L

IntechOpen

IntechOpen

